Research Article

Abdul Aabid*, Mohammed Abdulla, Meftah Hrairi and Muneer Baig

Optimizing piezoelectric patch placement for active repair of center-cracked plates

https://doi.org/10.1515/jmbm-2025-0089
Received October 1, 2025; accepted October 24, 2025;
published online December 9, 2025

Abstract: Active repair using piezoelectric materials offers a promising direction for extending the service life of cracked structural components. Conventional methods typically employ multiple patches placed around the crack, but such layouts may not deliver maximum efficiency. In this work, a different strategy is examined by bonding a single piezoelectric material patch directly across the crack line of a plate. A coupled finite element analysis in ANSYS is used to study how this placement influences stress intensity factor (SIF) and overall repair performance. The results highlight the critical role of patch location when bonded on the crack and energized by an electric field, the piezoelectric patch produces a markedly greater reduction in SIF compared to patches placed around the crack. This demonstrates the effectiveness of direct-on-crack placement in suppressing crack growth and emphasizes the need for careful consideration of patch positioning in active repair design. The study contributes new guidance for applying piezoelectric materials in structural repair and damage control.

Keywords: finite element method; stress intensity factor; piezoelectric; aluminum alloy; cracked plate

1 Introduction

Active repair using piezoelectric materials has emerged as a groundbreaking approach in structural engineering, aiming to enhance the integrity and longevity of damaged components [1]. The unique electromechanical properties of Lead Zirconate Titanate (PZT) enable real-time adjustments to structural dynamics and stress distributions, making them ideal for applications in the aerospace and automotive industries. Previous studies have successfully employed PZT patches in various configurations to mitigate crack propagation and improve the structural performance of thin-walled aluminum plates [2, 3]. For instance, Providakis et al. [4] studied the repair of a cracked cantilever structure subjected to varying external loads using FE modelling. Liu [5] investigated a cantilever beam with a central crack repaired using PZT patches mounted below the crack. The application of an external electric field to the PZT patches resulted in crack closure [6]. These results indicate that the PZT can generate stress through the coupling nodes, which may result in controlling the crack.

Duan et al. [7] addressed the issue of shear stress singularity at the delamination fracture point using a numerical method. A delaminated structure was restored using PZT material, and its effectiveness is measured by calculating the difference in shear stress near the delamination zone [8]. Platz et al. [9] managed to reduce the SIF in the cracked thin aluminium structure using an experimental approach. By applying a 100 V voltage to the PZT patches, they successfully facilitated crack mitigation. A PZT sensor was employed to assess the severity of the stress near the crack zone of a centre-cracked beam, while a PZT actuator was utilized to generate a bending moment to restore the beam's original structural position [10]. Abuzaid et al. [11] established an analytical model for a cracked plate repaired using a PIC151 patch with an aim to minimize the stress concentration. The influence of adhesive shear modulus on the actively repaired structure was studied by Abuzaid et al. [12] using a 3D finite element (FE) analysis approach. The utilization of a PZT patch was employed to mitigate stress concentration near a hole in a rectangular plate via numerical methods. Optimal placement of the PZT patch was explored, with validation against experimental data demonstrating strong agreement with numerical findings [13].

Abuzaid et al. [14] developed an analytical framework to assess the Mode-I crack behaviour in structural components.

***Corresponding author: Abdul Aabid**, Department of Engineering Management, College of Engineering, Prince Sultan University, Riyadh 11586, Saudi Arabia, E-mail: aaabid@psu.edu.sa. https://orcid.org/0000-0002-4355-9803
Mohammed Abdulla and Meftah Hrairi, Department of Mechanical and Aerospace Engineering, Kulliyyah of Engineering, International Islamic University Malaysia, Kuala Lumpur, Malaysia,
E-mail: hafizabdulla2426@gmail.com (M. Abdulla), meftah@iium.edu.my (M. Hrairi)
Muneer Baig, Department of Engineering Management, College of Engineering, Prince Sultan University, Riyadh 11586, Saudi Arabia

Their model integrated the principle of superposition to accurately calculate SIF, incorporating both the induced compressive stresses from PZT materials and external loading effects. Abuzaid et al. [15] conducted an experimental investigation on enhancing structural integrity by minimizing SIFs through active repair of edge-cracked configurations. The study involved bonding patches using Araldite adhesive and employing an E–413 piezo amplifier for PZT actuation. Hai [16] employed an analytical method to perform the repair of a multi-cracked beam using PZT patches. The analytical results were then validated using the FE method, and the displacement of the beam was controlled using the actuation of PZT. The effect of adhesive curing temperature on the repair performance of actively repaired aluminium plate was studied by [17] using Finite element analysis. Furthermore, the study was continued by [18] to study the influence of positive and negative temperature on repair efficiency along with parametric variations. In a recent study, active repair using a PZT patch has also been found through optimization techniques such as the Taguchi method [19], fuzzy logic [20], and machine learning [21].

Recent independent research has broadened and deepened the state of the art in piezoelectric-enhanced crack repair. Pattanayak et al. [22] used ABAQUS-based FE modeling on bottom-edge cracked I-beams, showing a 16–17 % reduction in SIF with 500 V actuation and an impressive 70 % extension in fatigue life, along with 2.9 % improved load capacity, demonstrating the promise of active repair under cyclic loading. In structural plates featuring circular-hole–initiated cracks, Konda et al. [23] found that rectangular piezoelectric patches, especially when applied on both faces, significantly reduce SIF under tensile loads; the most effective designs depend on geometry, placement, and polarization voltage. Aabid et al. [21] further investigated thin-walled aluminum plates with center cracks, illustrating via FE modeling that bonded PZT actuators can effectively mitigate Mode I crack propagation with SIF reductions validated under plane-stress conditions. Meanwhile, Aabid et al. [19] applied Taguchi optimization to piezoelectric patch-based repair on aluminum plates, identifying key parameter combinations that benchmark SIF reduction efficiency across patch dimensions, adhesive attributes, and applied voltage.

These examples spanning diverse geometries, loading conditions, and optimization techniques reinforce the expanding applicability of piezoelectric actuation in passive and active crack mitigation strategies for the repair of aluminum material structures. The novelty of this study lies in its approach of bonding a single PZT patch directly onto the crack in a thin-walled plate under plane stress conditions, contrasting with the conventional method of using two patches positioned around the crack. This configuration not only simplifies the repair process but also targets the root of the crack, potentially enhancing the efficiency of the repair. Utilizing ANSYS for FE analysis, the study systematically compares the outcomes of this innovative approach with the established configurations. By doing so, this research aims to contribute valuable knowledge to the field of active repair using piezoelectric materials.

2 Problem definition

The study models a center-cracked aluminum plate (height H = 160 mm, width 2 W = 100 mm, thickness T = 1 mm; crack length 2a) repaired with a bonded PIC151 PZT actuator using FM73 adhesive. The plate is subjected to a uniform tensile load of 1 MPa applied at both ends. The novelty lies in bonding a single PZT patch directly across the crack tip and comparing its performance with a conventional configuration of two patches placed symmetrically around the crack. Piezoelectric actuation is applied through the PIC151 patch to actively mitigate crack effects.

2.1 Geometrical model: pzt patches bonded around the crack

In this conventional setup, two PZT patches are bonded around the crack at a distance of 1 mm from the crack tip. Each PZT patch has dimensions of height Hp = 20 mm, width Wp = 40 mm, and thickness Tp = 0.5 mm. The patches are adhered to the plate using an adhesive layer with dimensions of height Had = 20 mm, width Wad = 40 mm, and thickness Tad = 0.03 mm. This configuration, as depicted in Figure 1, aims to generate compressive stress around the crack tip, thereby reducing the SIF and controlling crack propagation.

2.2 Geometrical model: pzt patch bonded directly on the crack

In the proposed novel configuration, a single PZT patch is bonded directly on top of the crack. The PZT patch dimensions remain the same as in the previous configuration (Hp = 20 mm, Wp = 40 mm, Tp = 0.5 mm), as do the adhesive layer dimensions (Had = 20 mm, Wad = 40 mm, Tad = 0.03 mm). The primary goal of this configuration, depicted in Figure 2, is to directly target the crack tip, with the potential to enhance repair efficiency by focusing the compressive stress precisely on the crack location.

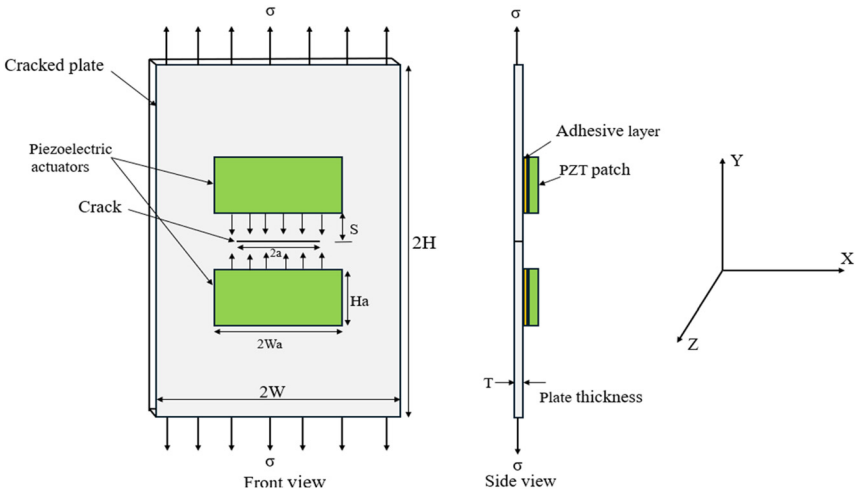

Figure 1: Damaged plate with PZT patch around the crack.

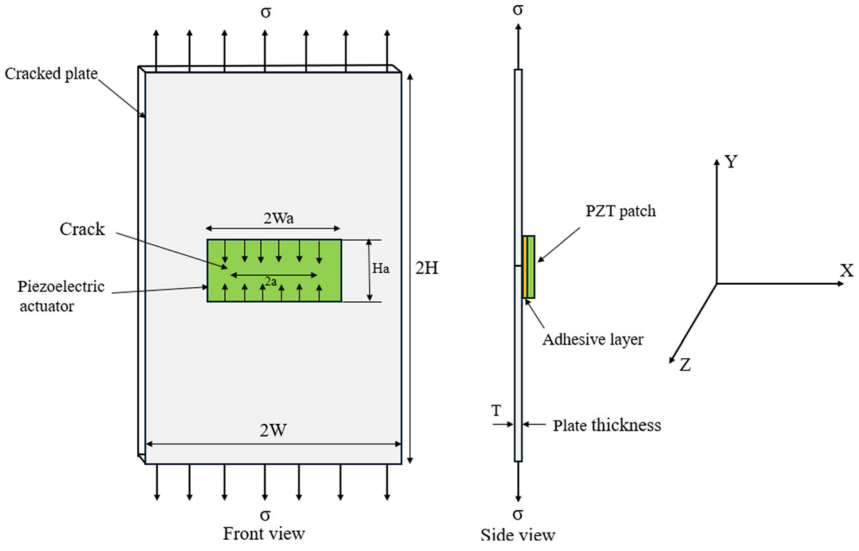

Figure 2: Damaged plate with PZT patch on the crack.

The material properties for the cracked plate, adhesive, and piezoelectric patch are tabulated in Table 1.

2.3 Boundary conditions and assumptions

Figure 3 shows how the boundary conditions were applied for both cases of PZT patch placement. In Figure 3(a), the PZT patch is bonded around the crack, while in Figure 3(b), it is bonded directly on the crack. The plate edges are fixed at the top and loaded with a uniform tensile stress (σ) at the bottom. The adhesive layer (Ta) and PZT patch (Tp) are clearly indicated in side views, showing their bonding thickness and interaction with the aluminum plate. This setup simulates realistic loading and constraint conditions during active repair.

To establish a consistent baseline for the electromechanical repair analysis, the model assumes perfect interfacial bonding, uniform electric field distribution, and linear piezoelectric behavior of the actuator material. These assumptions enable clear isolation of the coupling effects between the mechanical load and electric actuation. However, it is

Table 1: Selected materials properties [21].

Parameters	Cracked plate	PZT actuator	Adhesive
Density (kg/m^3)	2,715	7,800	–
Young's modulus (GPa)	68.95	–	1.83
Poison's ratio	0.33	–	0.32
Shear modulus (GPa)	–	–	0.96
Compliance matrix (m^2/N)	–	S11 = 15.0 × 10-12 S33 = 19.0 × 10-12	–
Electric permittivity coefficient	–	ε^T11 = 1,977 ε^T_{33} = 2,400	–
PZT strain coefficient (m/V)	–	d31 = −2.10 × 10-10 d32 = −2.10 × 10-10	–

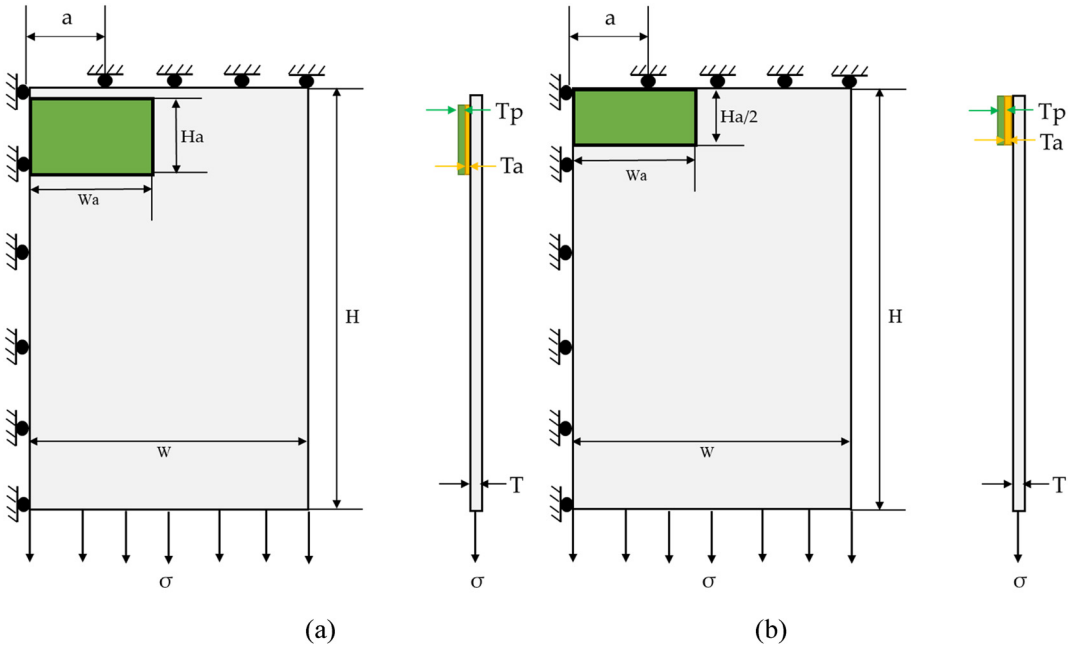

Figure 3: Boundary conditions applied to the model (a) around and (b) on the crack.

recognized that bond layer degradation, adhesive nonlinearity, and electric field edge effects may occur in real structures and could slightly influence the repair efficiency [6].

3 Computational fracture analysis

To compute the Mode-I SIF, we used the displacement extrapolation method in ANSYS KCALC command, consistent with standard LEFM practice and prior work on PZT-assisted crack repair. Quarter-point singular elements were placed at the crack tip to reproduce the $1/\sqrt{r}$ stress/strain singularity.

Based on the Figure 4 the origin at the tip, x,u along the crack, y,v normal to the crack; radial direction r and angle θ; nodes 1–3 along the crack face used for extrapolation ($\theta = 0°$). This exactly mirrors the procedure summarized above and in Abuzaid et al. [24].

ANSYS workflow-consistent.

- Set x along the crack plane and y normal to it, with the tip at the origin.
- Create a path beginning at the tip and continuing a few element lengths on each face.
- Use the first three nodes ahead of the tip ($\theta = 0°$ line) for extrapolation (see Figure 4: nodes 1–3).

The near tip opening displacement satisfies the LEFM linearization.

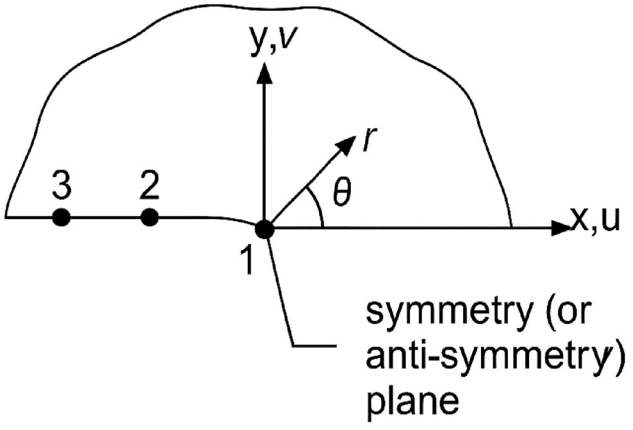

Figure 4: Typical crack face path for half-crack model.

$$\frac{|v|}{\sqrt{r}} = A + B\,r \tag{1}$$

so that as $r \to 0$ the intercept A and B are the parameters that obtained from the three nodal pairs (r_i,v_i) and it is depending on the geometry and load on the specimen. The SIF K_I is then computed from this extrapolated value using the standard LEFM proportionality used in Abuzaid et al. [24], which underpins the KCALC implementation.

$$K_I = \sqrt{2\pi}\,\frac{2\mu A}{1+K} \tag{2}$$

Current investigation used ANSYS APDL commercial code to calculate SIF with reasonable accuracy. The displacement

near the crack tip is obtained from FE simulations, and then the SIF is obtained based on the Eqn. [2].

3.1 FE modeling of the integrated structure piezoelectric

For the analysis in the new paper on active repair, the commercial finite element software ANSYS was employed, where three distinct bodies were modelled: the cracked plate, adhesive, and PZT patch. The cracked plate and adhesive were modelled using SOLID186 elements, which are 20-node higher-order elements suitable for 3D simulations, offering improved accuracy in capturing structural behaviour. The piezoelectric patch, however, was modelled using SOLID226 elements, which also have 20 nodes but incorporate up to six degrees of freedom per node, allowing seamless translation between mechanical and electrical properties, enabling the coupling required for active repair simulations.

A total of 15,146 elements were used for the cracked plate, 2,500 elements for the adhesive, and 5,000 elements for the PZT patch. The region around the crack tip was carefully refined using the KSCONC command to concentrate the key point of the crack tip, ensuring accurate computation of the SIF at the fracture point. The mesh was finely adjusted, with 10 elements placed around the circumference of the crack tip to capture the rapid changes in the stress and strain fields. Boundary conditions and external loads were applied, and the solution was obtained using the SOLVE command. To measure the SIF accurately, the displacement extrapolation method was applied, focusing on the displacements of nodes near the fracture tip. This approach is critical due to the rapid variation of stress and strain fields in the vicinity of the crack. Figure 5(a) and (b) depict the meshed model of the repaired structure for both cases where a PZT patch is bonded around the crack and a PZT patch is bonded on the crack, respectively.

3.2 Mesh convergence study

To ensure numerical accuracy, the mesh was refined around the crack tip using the KSCONC command to generate quarter-point singular elements. The plate was discretized with 15,000 elements, the adhesive with 2,500 elements, and the PZT actuator with 5,000 elements. A convergence study showed that beyond these mesh densities, the change in computed SIF was less than 2 %, confirming adequate accuracy. At least 10 elements were maintained around the crack front to capture the stress singularity field [6]. In addition to global convergence, graded mesh densities were employed, with the smallest elements concentrated around the crack tip region

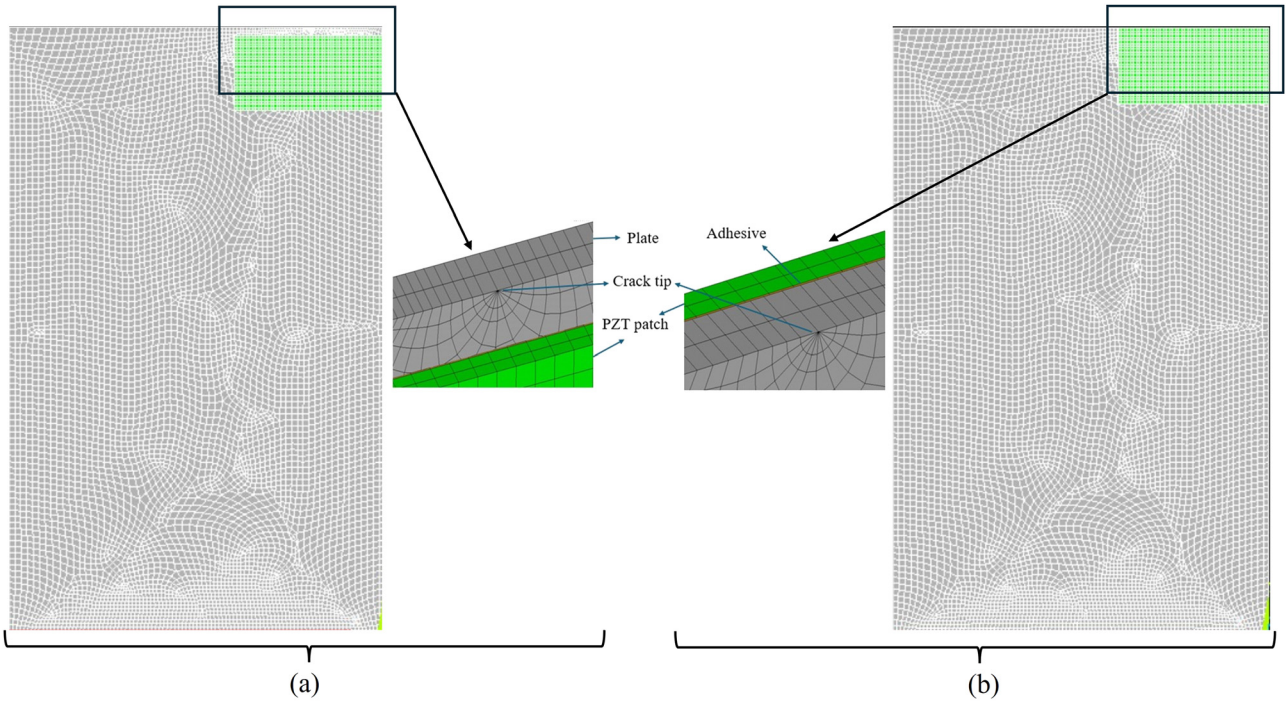

Figure 5: Mesh model with PZT patch bonded (a) around the crack, (b) on the crack.

(=0.05 mm, corresponding to about 9 % of the crack length) and gradually coarser elements (up to 1 mm) toward the outer regions. The influence of regional mesh variation on the SIF was also examined and found to cause less than 2 % difference in results, confirming that localized refinement adequately captured the stress singularity while maintaining overall mesh efficiency.

3.3 Validation of simulation models

3.3.1 Without the PZT patch

For the unrepaired edge-cracked plate, the FE results agree closely with both the closed-form LEFM solution and the reference experiment work. The relative errors are 2.20 % versus theory and 2.11 % versus experimental work (Table 2). These small deviations fall well within typical validation tolerances for crack-tip simulations of less than 3 %. The slight underprediction is conservative and likely stems from standard discretization and boundary-condition idealizations. Overall, the model provides a reliable baseline for reporting subsequent SIF-reduction (%) in the repaired cases. Theoretical data have been obtained from Tada's relation of edge-edge-cracked plate [25].

$$K_{I,\,\text{unrepaired}} = \sigma\sqrt{\pi a}\sqrt{\frac{2b}{\pi a}\tan\frac{\pi a}{2b}}\;\frac{0.752 + 2.02\left(\frac{a}{b}\right) + 0.37\left(1 - \sin\frac{\pi a}{2b}\right)^3}{\cos\frac{\pi a}{2b}} \tag{3}$$

where $K_{I,\text{unrepaired}}$ represent the Mode I SIF for the unpatched plates, a denotes the length of the crack (=10 mm), b denotes the breadth of the cracked plate (=40 mm), and σ denotes the uniaxial uniform load (=1 MPa).

3.3.2 With the PZT patch around the crack

The validation compares present FE results for an edge-cracked plate with existing experimental data at a voltage range of 20–80 V, illustrated in Table 3. The plate has been modeled based on the experimental work conducted by Abuzaid et al. [15], which has a height of 220 mm, of 38.5 mm width, 1 mm thickness with a crack length of 8.35 mm under an uniaxial uniform load of 1 MPa. All values of SIFs are normalized by $\sigma_{ext}\sqrt{\pi a}$ for comparison purposes and therefore the Table 3 results are unitless. In both, SIF decreases monotonically with voltage, confirming correct actuation physics. The FE model consistently overpredicts normalized SIF by 6.7–7.9 %, implying a conservative estimate of repair efficiency. The small but growing bias with voltage likely arises from idealizations: uniform electric field through the patch/adhesive, linear piezoelectric coefficients (d_{31}) without field dependence, perfect bonding and no shear-lag degradation, and nominal material properties. Additional sources include boundary-condition simplifications and neglect of fringing fields. Overall, agreement within 8 % supports model fidelity while highlighting avenues for refinement.

Table 2: Validation of current FE findings without the PZT patch.

Condition	SIF (MPa$\sqrt{\text{m}}$) – without repair
Theoretical [25]	0.18139
Experimental [15]	0.18122
Simulation (present work)	0.1774

Table 3: Validation of current FE findings with a PZT patch around the crack.

Applied voltage (V)	Normalized SIF experimental [15]	Normalized SIF SIF simulation (present work)	Relative error (%)
30	1.12	1.2	6.667
50	1.1	1.18	6.779
70	1.08	1.16	6.896
100	1.05	1.14	7.894

4 Results and discussion

4.1 SIF for different cases of PZT patch placement

Figure 6 demonstrates the significant impact of PZT patch placement on the efficiency of repairing a cracked plate under an applied electric field. The data underscores that the positioning of the PZT patch plays a pivotal role in stabilizing the crack and reducing the SIF.

When a PZT patch is positioned directly on the crack and actuated with an electric field, the SIF exhibits a significant reduction, particularly at longer crack lengths. A 100 V electric field applied to this actuator generates compressive stress, drawing the crack faces together. This results in a 75 % reduction in SIF compared to the unrepaired case, effectively inhibiting crack propagation as the applied compressive forces counteract the crack growth. Notably, as

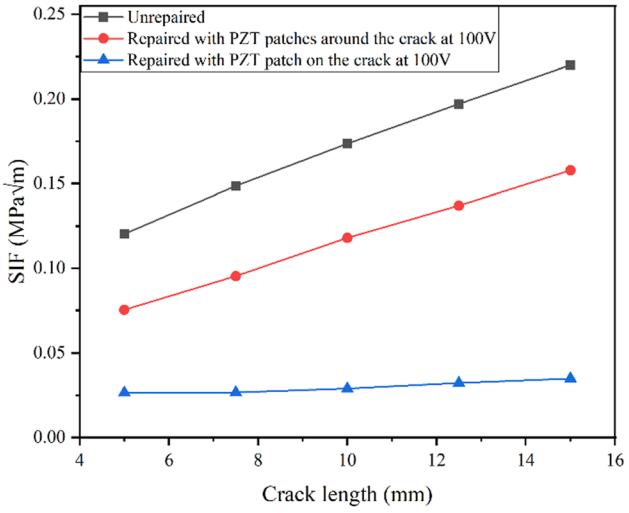

Figure 6: SIF for different positions of PZT patch placement.

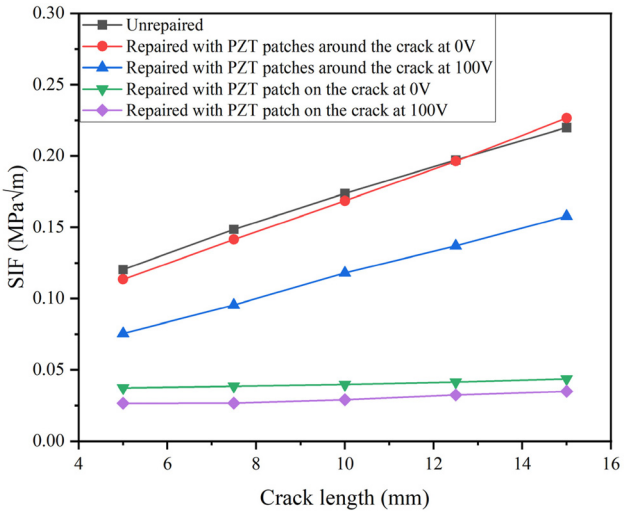

Figure 7: SIF under the active and passive effect of the PZT patch.

the crack length increases, the SIF stabilizes, showing asymptotic behaviour, which indicates that the patch effectively arrests the crack growth at higher crack lengths. This phenomenon demonstrates the superior performance of placing the patch directly over the crack for arresting crack propagation.

On the other hand, in cases where the PZT patches are placed around the crack, the SIF reduction is less pronounced. The electric field still reduces the SIF, but the effectiveness diminishes as the crack length increases. At shorter crack lengths (e.g., 5 mm), the reduction in SIF is around 38 %. However, as the crack grows, the percentage reduction in SIF steadily decreases; it reduces to 35 % for a 7.5 mm crack, 32 % for a 10 mm crack, 29 % for a 12.5 mm crack, and finally, 25 % for a 15 mm crack. As the crack length increases, the stress concentration at the crack tip becomes more dominant, and the patch's ability to mitigate SIF through indirect stress distribution weakens.

4.2 Active and passive effects of pzt patch placement on sif

The influence of PZT patch placement on the SIF during crack repair is critical in determining the effectiveness of the repair strategy. Various configurations of PZT patches, either placed around the crack or directly on the crack tip, both in passive (0 V) and active (100 V) states, have been discussed.

4.2.1 Passive repair scenario (0 V)

When PZT patches are placed around the crack without applying an electric field, they function passively. This placement provides some restraint against crack propagation but does not significantly reduce the SIF compared to the unrepaired case. The SIF reduction in this configuration is only 5.68 %, highlighting the limited ability of the patch to arrest the crack. The SIF increases nearly linearly with the crack length, indicating minimal control over crack propagation represented by the red line in Figure 7.

In contrast, placing the PZT patch directly on the crack tip enhances its ability to hold the crack closed, even without an electric field. This configuration shows a more pronounced reduction in SIF, achieving up to 67 % reduction, as the patch directly supports the crack, transferring stress from the host structure to the patch. This setup effectively reduces crack propagation, evident from the significantly lower SIF values compared to the patch-around-crack configuration represented by the green line in Figure 7.

4.2.2 Active repair scenario (100 V)

When an electric field of 100 V is applied, the PZT patches around the crack generate compressive stresses, which further reduce the SIF. However, the reduction is not as effective as when the patch is placed directly on the crack tip. The blue graph line in Figure 7 shows a noticeable, but not substantial, reduction in SIF with increasing crack length.

The most effective configuration for minimizing SIF is with the PZT patch placed directly on the crack tip and actuated with 100 V. This setup results in the most significant reduction in SIF, up to 75 % compared to the unrepaired case represented by the pink graph line in Figure 7. The electric field induces compressive stress in the PZT patch, effectively

closing the crack and preventing further propagation. This configuration ensures optimal stress concentration management at the crack tip, leading to better crack arresting capabilities.

4.3 Performance of PZT patches under increasing mechanical load

4.3.1 PZT patches placed around the crack

In the scenario where PZT patches are positioned around the crack and actuated with an electric field of 100 V, the study reveals a noticeable but diminishing impact on the reduction of the SIF as mechanical load increases, as illustrated in Table 4. The SIF reduction observed at a 1 MPa load was 38 %, which significantly decreased to 6.3 % at a 50 MPa load. This trend indicates that while PZT patches can initially reduce SIF effectively, their efficacy diminishes as the mechanical load increases. This reduction in SIF efficacy could be attributed to the fact that PZT patches placed around the crack may not fully arrest crack propagation. The patches generate a compressive stress towards the crack length that helps reduce SIF, but this effect is less localized compared to patches placed directly on the crack. As the mechanical load increases, the ability of these patches to influence the crack tip stress concentration diminishes, leading to less reduction in SIF.

4.3.2 PZT patch placed on the crack

Conversely, when a PZT patch is placed directly on the crack and actuated with an electric field of 100 V, the reduction in SIF remains significantly more consistent across increasing mechanical loads as listed in Table 5. The SIF reduction starts at 75 % for a 1 MPa load and gradually decreases to 68.3 % at a 50 MPa load, reflecting a much smaller decrease in effectiveness compared to the patches placed around the crack. This higher and more consistent reduction in SIF can be explained by the direct placement of the PZT patch, which allows it to exert compressive stress directly at the crack tip. The localized compressive stress generated by the PZT patch under an electric field effectively closes the crack, thereby significantly reducing SIF and impeding crack propagation. Even as mechanical load increases, the patch's ability to directly influence and reduce stress at the crack tip remains relatively stable, which explains the smaller reduction in efficacy compared to patches placed around the crack.

Table 4: SIF when PZT patches are placed around the crack under increasing mechanical load.

Unrepaired		Repaired	
Mechanical load (MPa)	SIF (MPa$\sqrt{m}$)	Mechanical load	SIF (MPa$\sqrt{m}$)
1	0.12025	1	0.07543
5	0.60126	5	0.5291
10	1.2025	10	1.0962
20	2.405	20	2.2303
30	3.6076	30	3.3645
40	4.8101	40	4.4987
50	6.0126	50	5.6328

Table 5: SIF when PZT patches are placed on the crack under increasing mechanical load.

Unrepaired		Repaired	
Mechanical load (MPa)	SIF (MPa$\sqrt{m}$)	Mechanical load	SIF (MPa$\sqrt{m}$)
1	0.12025	1	0.028162
5	0.60126	5	0.1598
10	1.2025	10	0.32672
20	2.405	20	0.72103
30	3.6076	30	1.1153
40	4.8101	40	1.5097
50	6.0126	50	1.904

4.4 Parametric investigation

The numerical results obtained from the FE method were further analyzed to study the influence of patch geometry, adhesive, and actuator parameters on the SIF. To ensure consistent comparison between the repaired and unrepaired specimens, the SIF reduction was expressed in percentage form rather than in absolute units in parametric investigation. This normalization eliminates the dimensional differences associated with individual SIF values and clearly highlights the effectiveness of the applied repair technique. The percentage reduction in Mode I SIF was determined using the following relation:

$$\text{SIF reduction } (\%) = \frac{K_{I,\,\text{unrepaired}} - K_{I,\,\text{repaired}}}{K_{I,\,\text{unrepaired}}} \times 100 \qquad (4)$$

where $K_{I,\,\text{unrepaired}}$ and $K_{I,\,\text{repaired}}$ represent the Mode I SIF for the unpatched and repaired plates, respectively. This formulation provides a dimensionless metric that simplifies result interpretation and allows straightforward comparison across different repair configurations.

4.4.1 Effect of applied voltage

A detailed parametric analysis was conducted by varying the applied voltage from 0 V to 100 V in increments of 10 V (Figure 8). The results confirmed a strong dependence of Mode I SIF reduction on the applied electrical potential, while also capturing the passive repair contribution at 0 V. When a patch was bonded directly on the crack tip, even without actuation, a significant 67 % reduction in SIF was achieved due to the passive stiffening effect of the bonded actuator. With increasing voltage, the reduction improved further, reaching 75 % at 100 V. In contrast, patches bonded around the crack showed only a minor passive effect of 6 % reduction at 0 V, which gradually increased to 20 % at 50 V, and 38 % at 100 V. These results demonstrate two important findings: first, the direct-on-crack placement provides substantial crack-arresting capability even in the passive state, which is absent in conventional configurations; second, while higher voltages enhance both repair strategies, the direct-on-crack configuration utilizes the electrical actuation far more effectively, achieving superior and stable SIF reductions across the entire voltage range.

4.4.2 Effect of patch thickness

A detailed parametric study was conducted by varying the PZT patch thickness at 0.25, 0.5, 0.75, and 1.0 mm (Figure 9). Although a 0.25 mm actuator is practically not feasible to manufacture or integrate due to handling and durability constraints, it was still considered in the simulation for comparison purposes and to better understand scaling

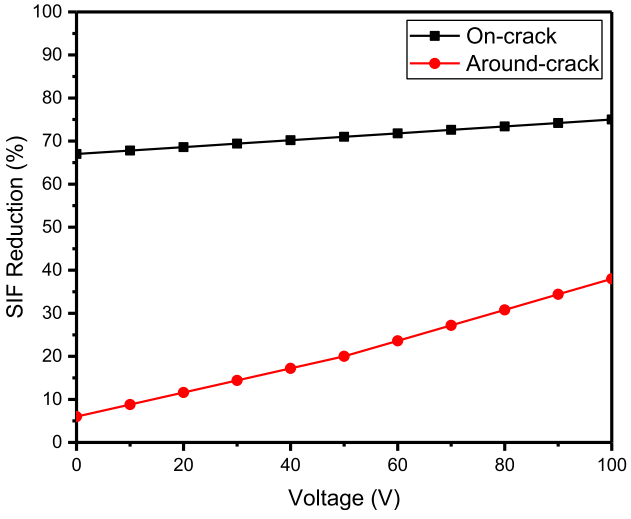

Figure 8: Effect of PZT patch voltage on SIF reduction.

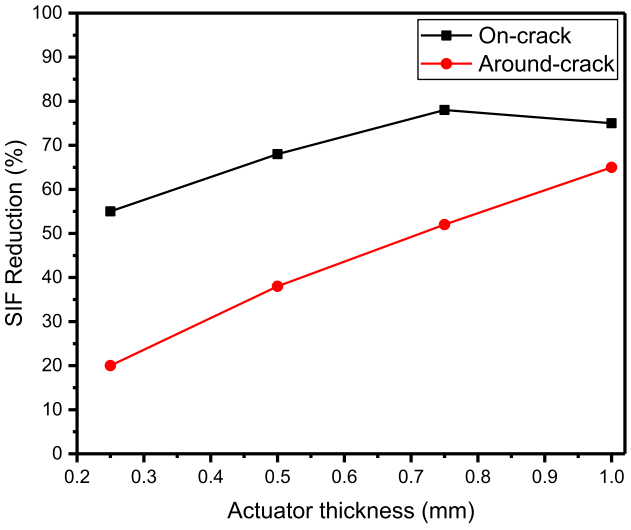

Figure 9: Effect of PZT patch thickness on SIF reduction.

effects. The results revealed distinct trends depending on the placement of the patch. When the PZT actuator was bonded around the crack, the reduction in SIF showed a monotonic increase with thickness. The improvement grew steadily from about 20 % at 0.25 mm to nearly 65 % at 1.0 mm, highlighting that thicker patches provide better load transfer and enhanced crack-closure stresses in this configuration.

In contrast, when the PZT actuator was placed directly over the crack tip, the behavior exhibited an optimum performance at 0.75 mm thickness, achieving a maximum SIF reduction of nearly 78 %. However, a sudden drop was observed at 1.0 mm thickness, with the reduction decreasing to approximately 75 %. This reversal indicates that beyond a certain thickness, the efficiency of stress transfer from the actuator to the substrate diminishes, limiting further improvement and in some cases reducing effectiveness. These findings suggest that while increasing patch thickness generally enhances repair performance when placed around the crack, careful optimization is required when positioning the actuator directly on the crack. Particularly, excessive thickness in the direct-on-crack configuration may lead to stress mismatch and reduced crack-closing efficiency.

In summary, the best SIF reduction was achieved at a PZT thickness of 0.75 mm, where the actuator stiffness closely matched that of the substrate, enabling optimal stress transfer and crack-closing compression. Beyond this thickness (1.0 mm), the increased stiffness of the patch caused stress-transfer inefficiency and partial load-sharing loss, resulting in a slight decrease in SIF reduction despite higher actuation capability.

4.4.3 Effect of crack length ratio with PZT width (a/W)

Keeping the crack length fixed at $2a = 20$ mm ($a = 10$ mm) and the actuation level the same across cases, the PZT actuator width varied to 30, 40, and 50 mm (Figure 10). The on-crack placement shows consistently higher mitigation and mild saturation: SIF reduction improves from 71 % (30 mm) to 75 % (40 mm) and 77 % (50 mm). The around-crack placement benefits more noticeably from added width, rising from 30 % (30 mm) to 38 % (40 mm) and 43 % (50 mm). Interpretation. Increasing the width enlarges the load-transfer region and the span over which compressive stresses oppose crack opening.

For around-crack patches, the extra width mainly increases shear-lag coupling through the adhesive and engages a larger ligament on either side of the crack, so the percentage reduction grows steadily. For on-crack patches, the crack faces are already strongly constrained; additional width still helps, but returns diminish beyond 40 mm because the local crack-closing work becomes limited by the available piezo stress at the same voltage (stiffness grows faster than useful imposed displacement), yielding only a small gain from 40 to 50 mm.

Meanwhile, it was observed that the SIF reduction improves as the patch width increases up to 50 mm. Beyond this value, the improvement becomes marginal, indicating that the width range of 40–50 mm provides an optimal balance between effective stress transfer and structural stiffness.

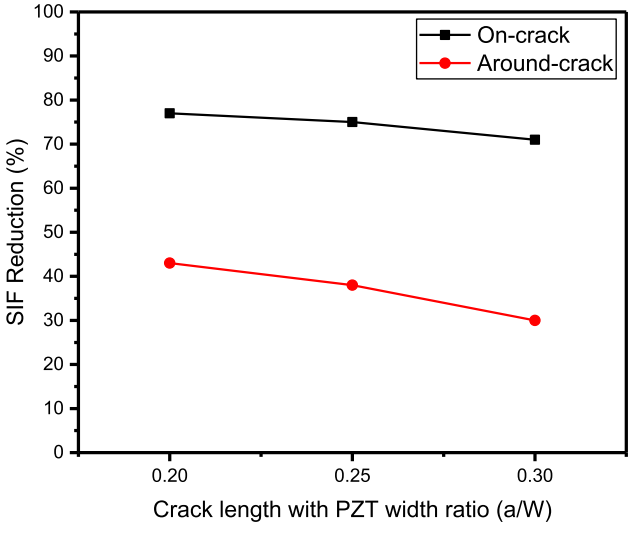

Figure 10: Effect of crack length with PZT width ratio (a/W) on SIF reduction.

5 Conclusions

This work confirms that where the PZT patch is bonded dominates repair performance. A single on-crack patch provides the greatest SIF reduction, delivering 67 % mitigation even without actuation and 75 % at 100 V, while remaining effective under high mechanical loads (68 % at 50 MPa). In comparison, around-crack patches offer smaller and load-sensitive benefits (38 % at 1 MPa to 6.3 % at 50 MPa). These outcomes are supported by a converged mesh and LEFM-consistent validation. The expanded parametric study clarifies practical design rules. First, the voltage sweeps show that on-crack placement uses actuation more efficiently, achieving strong reductions from moderate voltages; around-crack behavior saturates earlier. Second, thickness should be chosen with placement in mind: around-crack benefits monotonically up to 1.0 mm, but on-crack exhibits an optimum near 0.75 mm and a measurable drop at 1.0 mm, indicating stress-transfer limits at constant voltage. Third, with 2a = 20 mm, increasing actuator width from 30 to 50 mm steadily improves the around-crack case (30–38–43 %) and yields smaller, saturating gains on-crack (71–77 %). Together, these results recommend an on-crack layout actuated in the 50–100 V range, 0.5–0.75 mm thickness, and 40–50 mm width as a balanced, high-efficiency design envelope.

6 Limitation

Limitations include a single-crack configuration, ideal bonding assumptions, and primarily static loading in simulation. Future work will address fatigue and thermo-mechanical coupling, refine adhesive modeling (including imperfections), and pursue experimental validation to translate these guidelines into deployable repair procedures for aerospace and automotive structures.

Acknowledgments: This research is supported by the Structures and Materials (S&M) Research Lab of Prince Sultan University, and the authors acknowledge Prince Sultan University for paying the article processing charges (APC).
Funding information: Structures and Materials (S&M) Research Lab of Prince Sultan University.
Author contributions: All authors have accepted responsibility for the entire content of this manuscript and approved its submission.
Conflict of interest: Authors state no conflict of interest.

Data Availability Statement: The datasets generated during and/or analyzed during the current study are available from the corresponding author on reasonable request.

References

1. Aabid A, Hrairi M, Mohamed Ali SJ, Ibrahim YE. Review of piezoelectric actuator applications in damaged structures: challenges and opportunities. ACS Omega 2023;8:2844–60.
2. Wang Q, Quek ST, Liew KM. On the repair of a cracked beam with a piezoelectric patch. Smart Mater Struct [Internet] 2002;11:404–10.
3. Wang Q, Quek ST. Repair of delaminated beams via piezoelectric patches. Smart Mater Struct 2004;13:1222–9.
4. Providakis CP. Repair of cracked structures under dynamic load using electromechanical admittance approach. Key Eng Mater 2007;348–349:49–52.
5. Liu TJC. Crack repair performance of piezoelectric actuator estimated by slope continuity and fracture mechanics. Eng Fract Mech 2008;75:2566–74.
6. Aabid A, Hrairi M, Abuzaid A, Syed J, Ali M. Estimation of stress intensity factor reduction for a center-cracked plate integrated with piezoelectric actuator and composite patch. Thin-Walled Struct [Internet] 2021;158:107030.
7. Duan WH, Quek ST, Wang Q. Finite element analysis of the piezoelectric-based repair of a delaminated beam. Smart Mater Struct [Internet] 2008;17:015017.
8. Wu N, Wang Q. Repair of a delaminated plate under static loading with piezoelectric patches. Smart Mater Struct 2010;19:105025.
9. Platz R, Stapp C, Hanselka H. Statistical approach to evaluating reduction of active crack propagation in aluminum panels with piezoelectric actuator patches. Smart Mater Struct 2011;20:085009.
10. Wu N, Wang Q. An experimental study on the repair of a notched beam subjected to dynamic loading with piezoelectric patches. Smart Mater Struct [Internet] 2011;20:115023.
11. Abuzaid A, Hrairi M, Dawood MS. Mode I stress intensity factor for a cracked plate with an integrated piezoelectric actuator. Adv Mater Res [Internet] 2015;1115:517–22.
12. Abuzaid A, Dawood MS, Hrairi M. Effects of adhesive bond on active repair of aluminium plate using piezoelectric patch. Appl Mech Mater [Internet] 2015;799–800:788–93.
13. Fesharaki JJ, Madani SG, Golabi S. Effect of stiffness and thickness ratio of host plate and piezoelectric patches on reduction of the stress concentration factor. Int J Adv Struct Eng 2016;8:229–42.
14. Abuzaid A, Hrairi M, Dawood MSIS. Modeling approach to evaluating reduction in stress intensity factor in center-cracked plate with piezoelectric actuator patches. J Intell Mater Syst Struct 2016;28:1–12.
15. Abuzaid A, Hrairi M, Dawood MS. Experimental and numerical analysis of piezoelectric active repair of edge-cracked plate. J Intell Mater Syst Struct 2018;29:3656–66.
16. Hai TT. Static repair of multiple cracked beam using piezoelectric patches. Vietnam J Mech 2021;43:197–207.
17. Abdulla M, Hrairi M, Aabid A, Abdullah NA. Finite element analysis of a repaired cracked aluminium plate with piezoelectric patches under mechanical and thermal loading. J Adv Res Appl Sci Eng Technol. 2025;1:171–83.
18. Abdulla M, Hrairi M, Aabid A, Abdullah NA, Baig M. Comparative analysis of active bonded piezoelectric repair systems for damaged structures under mechanical and thermo-mechanical loads. Actuators 2024;13:390.
19. Aabid A, Hrairi M, Ali JSM. Optimization of damage repair with piezoelectric actuators using the taguchi method. Frat Ed Integrità Strutt 2024;67:137–52.
20. Aabid A, Hrairi M, Raheman MA, Ibrahim YE. Enhancing aircraft crack repair efficiency through novel optimization of piezoelectric actuator parameters: a design of experiments and adaptive neuro-fuzzy inference system approach. Heliyon [Internet] 2024;10:e32166.
21. Aabid A, Baig M, Malik MA. Enhancing piezoelectric control of cracks in thin solid aluminum plates using finite element data and a neural networks approach. AIP Adv 2025;15:13.
22. Pattanayak S, Roy G, Pohit G. A novel approach to enhance the structural integrity of a bottom-edge cracked I-beam with piezoelectric actuators. Mech Adv Mater Struct [Internet] 2024;0:1–20.
23. Konda GK, Schuster J, Shaik YP. Enhancing stress intensity factor reduction in cracks originating from a circular hole in a rectangular plate under uniaxial stress through piezoelectric actuation. Mater Sci Appl 2024;15:1–14.
24. Abuzaid A, Hrairi M, Dawood MS. Modeling approach to evaluating reduction in stress intensity factor in center-cracked plate with piezoelectric actuator patches. J Intell Mater Syst Struct [Internet] 2017;28:1334–45.
25. Tada H, Paris PC, Irwin GR. The stress analysis of cracks handbook. 3rd ed. [Internet] 2000. Available from: http://ebooks.asmedigitalcollection.asme.org/book.aspx?bookid=230.